

# Mechanisms of dark matter genesis

Chmykhalo Dmitry

# TABLE OF CONTENT

<b>Introduction</b>	<b>2</b>
<b>1 Genesis of dark matter</b>	<b>3</b>
<b>2 Freeze-In During an Early MD Era</b>	<b>7</b>
2.1 Freeze-In during Non-Adiabatic evolution . . . . .	11
<b>3 Non-thermal production</b>	<b>13</b>
<b>4 Cannibal Dark Matter</b>	<b>18</b>
<b>References</b>	<b>21</b>

# INTRODUCTION

The generation of DM in the early universe can proceed via thermal or non-thermal production, or both, or it may result from a particle-antiparticle asymmetry. None of the mechanisms proposed below explains the approximate relation

$$\rho_{B,0} = \rho_{DM,0}, \tag{1}$$

where  $\rho_{B,0}$  and  $\rho_{DM,0}$  energy density of baryons and dark matter particles in the modern Universe. This approximate equality was also fulfilled in the past, at rather late stages of the expansion of the Universe. Several possible mechanisms for the generation of dark matter and baryon asymmetry have been proposed in the literature, leading to the relation 1.1. However, a convincing and natural explanation for the approximate coincidence has not yet been found. Perhaps this is indeed a coincidence.

# 1. GENESIS OF DARK MATTER

**Freeze-out:** The process of chemical decoupling from the high-temperature, high-density thermal bath (freeze-out) as a paradigm for particle production in the early universe is both a predictive and a successful one. The possibility that just like light elements, neutrinos, and CMB photons, particle DM also originated from a thermal decoupling process has thus garnered significant attention.

A particle species chemically decouples when the rate for the species' number-changing processes drops below the Hubble rate  $H$ . Rough estimates for the abundance of relics can be obtained by calculating the freeze-out (i.e. “decoupling”) temperature  $T_{f.o.}$ , corresponding to  $H(T_{f.o.}) \sim (T_{f.o.})$ , equating the comoving number density at freeze-out and today, eventually obtaining the physical density of relic particles today. This procedure assumes that entropy is conserved between  $T_{f.o.}$  and today, an assumption that could well be violated, especially for heavy relics that decouple early, for instance by entropy injection episodes. Notice also that the freeze-out calculation strongly depends on the assumed background cosmology, and changes e.g. if the early universe is not radiation-dominated around DM decoupling.

The calculation of the freeze-out relic abundance hinges on a Boltzmann equation relating the Liouville operator to the collision operator acting on the phase space density. Under a variety of simplifying assumptions including homogeneity and isotropy, it is possible to reduce the relevant equation for the number density  $n$  of a single species pair-annihilating with particles in the thermal bath via 2-to-2 processes to

$$\frac{dn}{dt} - 3Hn = -\langle\sigma v\rangle(n^2 - n_{eq}^2), \quad (1.1)$$

where  $\langle\sigma v\rangle$  is the thermally-averaged pair-annihilation cross section times relative velocity, and  $n_{eq}$  is the equilibrium number density. Relics for which the freeze-out temperature is much larger than the particle mass (and thus that freeze-out as ultra-relativistic) are called hot relics; if the opposite is true, the

relic is instead considered cold.

A straightforward calculation shows that to leading order the frozen-out density of hot relics is linearly proportional to the relic particle mass. The comoving number density  $Y = n/s$ , where  $s$  is the entropy density, for a hot relic is approximately given by its equilibrium value,

$$Y_{f.o.} \simeq Y_{eq} \simeq 0.278 \frac{g_{eff}}{g_{*s}}, \quad (1.2)$$

where  $g_{eff}$  is the relic's effective number of degrees of freedom, and  $g_{*s}$  is the number of entropic relativistic degrees of freedom, both calculated at  $T_{f.o.}$ . The resulting relic abundance, assuming an iso-entropic expansion, is

$$\Omega_{hot} h^2 = \frac{m Y_{f.o.} s_0 h^2}{\rho_0} \simeq \frac{m}{93 \text{ eV}}, \quad (1.3)$$

with  $s_0$  the entropy density today, and with the latter equality holding for the case of SM neutrinos, with a freeze-out temperature around 1 MeV (which enters in the final relic abundance through the degrees of freedom dependence on the right-hand-side of Eq. (1.3)).

For cold relics, the leading-order dependence of the relic abundance on the DM particle properties is an inverse proportionality relation to the pair-annihilation cross section,

$$\Omega_{cold} h^2 \simeq 0.1 \left( \frac{x_{f.o.}}{20} \right) \left( \frac{10^{-8} \text{ GeV}^{-2}}{\sigma_{DM+DM \leftrightarrow DM}} \right), \quad (1.4)$$

where  $x \equiv m_{DM}/T$ . In turn, the freeze-out temperature is approximately given by the solution to the equation

$$\sqrt{x} \cdot e^{-x} = (m_{DM} \cdot M_P \cdot \sigma_{DM+DM \leftrightarrow DM})^{-1}, \quad (1.5)$$

where  $M_P \simeq 2.43510^{18} \text{ GeV}$  is the reduced Planck mass. As a result,  $T_{f.o.} \simeq m_{DM}/x_{f.o.}$ , with  $x_{f.o.}$  a number between 10 and 50, depending on the cross section, with only a logarithmic dependence on the DM mass. Since for electroweak-scale cross sections and masses  $\sigma_{DM+DM} \simeq 10^{-8} \text{ GeV}^{-2}$ , “weakly-interacting massive particles”, or WIMPs have gained exceptional popularity. Notice that Eq. (1.4) bears, however, no connection to the weak scale, despite the relation being known as “WIMP miracle”.

Numerous scenarios exist, including notably supersymmetry and models with universal extra dimensions where the relic abundance of the DM is controlled by processes involving a slightly heavier, unstable, co-annihilating species. In this case the calculation of the abundance of the stable species proceeds similarly to what outlined above, with an effective pair-annihilation cross section that captures the effects of co-annihilation replacing the pair-annihilation cross section.

**Freeze-in:** Collisional processes can lead to the production of out-of-equilibrium particles that progressively accumulate over cosmic time, a process sometimes called freeze-in. The abundance of the frozen-in particles produced at a given redshift depends on the product of the production rate times the Hubble time at that redshift. Freeze-in generally implies that the lightest observable sector particles decay to the DM with relatively long lifetimes, giving peculiar signals at colliders. Gravitinos are an example of DM candidates possibly produced via a freeze-in type scenario, albeit the portal coupling is in that case via a higher dimensional, Planck-suppressed operator.

**Cannibalization and other dark-sector number-changing processes:** Thermal processes can drive the abundance of the DM beyond simple 2-to-2 number-changing interactions. For instance, DM can “cannibalize” itself if  $n \rightarrow 2$  processes exist. In this case, a critical aspect is whether or not the DM sector is in thermal contact with the Standard Model thermal bath. If it is,  $n \rightarrow 2$  processes can drive the relic abundance, e.g. in the Strongly Interacting Massive Particles (SIMP) scenario. Models exist where the kinetic decoupling (i.e. the decoupling from the thermal equilibrium velocity distribution) of the two sectors drives the abundance of the DM (elastically decoupling relics, or ELDERS). When the two sectors are not in thermal contact,  $n \rightarrow 2$  processes heat the DM sector dramatically, rapidly affecting the temperature ratio between the visible and dark sectors. If the relevant cross sections are large enough, and the DM mass light enough, significant effects can arise in structure formation.

**Non-thermal production:** DM production can proceed via processes out of thermal equilibrium (“non-thermal” production). These include DM production via the decay of a “mother” particle (or of topological defects, moduli etc.) to the DM, or production via gravitational effects.

**Asymmetric DM:** An enticing alternative possibility for DM production is that of asymmetric DM: the relic DM abundance arises from an asymmetry between anti-DM and DM. This asymmetry may or may not be related to the baryon-antibaryon asymmetry. If it is, then depending on the model and its thermal history, a relation exists between the mass of the DM and the proton mass. A variety of proposals have been put forward where alternately baryogenesis is explained from a DM sector asymmetry, or vice-versa.

**Primordial Black Holes production:** A qualitatively stand-alone class of DM candidates, primordial black holes (PBHs), arises from entirely different mechanisms from what reviewed above. PBHs are thought to originate from gravitational collapse of large density fluctuations in the early universe. The over-densities could be produced in a variety of ways, such as topological defects like cosmic strings, necklaces or domain walls, curvature fluctuations from a period of ultra-slow-roll, a sound speed “resonance” , an early phase of matter domination, or subhorizon phenomena including a phase transition and preheating. Albeit the calculation depends on the details of gravitational collapse, the formation time is connected to the PBH mass via  $M = \gamma \dot{M}_{PBH} \simeq 2 \cdot 10^5 \gamma \dot{M}$  with  $\gamma \simeq (1/\sqrt{3})^3$  during radiation domination.[1]

## 2. FREEZE-IN DURING AN EARLY MD ERA

Dark matter,  $X$ , may be generated by new physics at the TeV scale during an early matter-dominated (MD) era that ends at temperature  $T_R \ll \text{TeV}$ . Compared to the conventional radiation-dominated (RD) results, yields from both Freeze-Out and Freeze-In processes are greatly suppressed by dilution from entropy production, making Freeze-Out less plausible while allowing successful Freeze-In with a much larger coupling strength. Freeze-In is typically dominated by the decay of a particle  $B$  of the thermal bath,  $B \rightarrow X$

When inflation ended, provided the inflaton decays were not extremely rapid, there was an era of matter domination (MD) which ended at the reheat temperature  $T_R$ . It is commonly assumed that  $T_R$  is very high, many orders of magnitude above the TeV scale, but observationally the most stringent constraints are from the effective number of neutrino species,  $T_R > 4 \text{ MeV}$ . This early MD era could extend for many decades in temperature above  $T_R$ , and include the TeV epoch. There are several alternative origins for a long early MD era, including long-lived heavy particles that were once in thermal equilibrium and oscillating fields composed of light bosons. When the MD era results from inflation it has an evolution that is purely Non-Adiabatic in character, giving a  $MD_{NA}$  era. The more general MD era splits into two, beginning with Adiabatic evolution,  $MD_A$ , and ending with  $MD_{NA}$ , as illustrated in Fig. 2.1.

Particle dark matter requires an addition to the Standard Model with a cosmologically stable particle  $X$  of mass  $m_X$ . How is the abundance of  $X$  determined? The Freeze-Out mechanism results if  $X$  has sufficient interactions with the known particles that it is in thermal equilibrium at temperatures  $T$  of order  $m_X$ . As  $T$  drops below  $m_X$ ,  $X$  tracks a Boltzmann distribution for a while but, as it becomes more dilute, its annihilation rate drops below the expansion rate and it freezes out of thermal equilibrium. This mechanism has great generality, applying to a wide range of theories where the interactions of  $X$  are sufficient to put it in thermal equilibrium at  $T \sim m_X$ . Furthermore, it

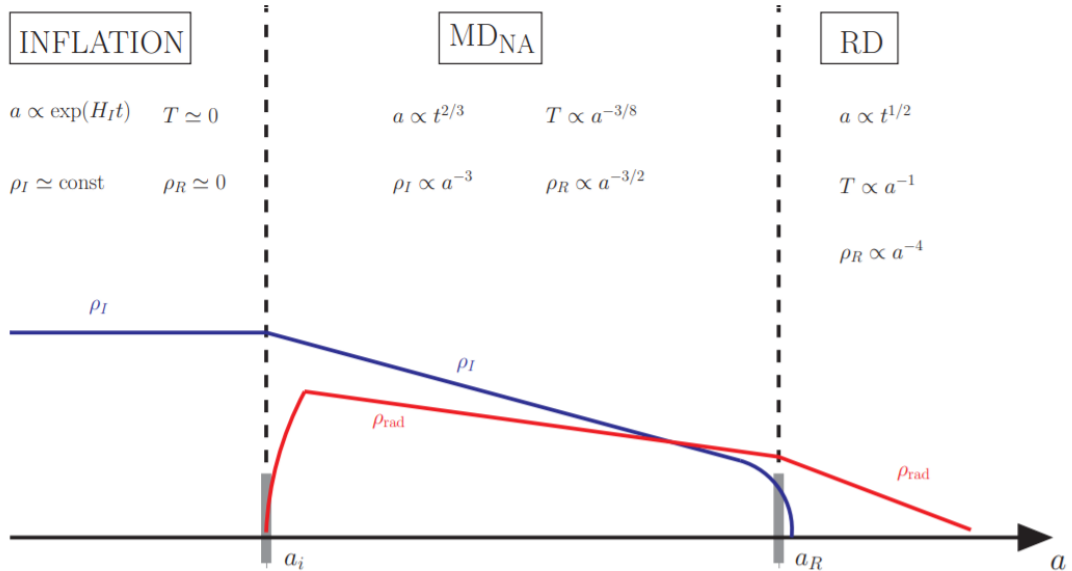


Figure 2.1: A long MD era after inflation

is highly predictive since it is an IR dominated process - it does not depend on any physics at energy scales above its mass. Indeed, Freeze-Out during the RD era suggests  $m_X$  is broadly of order a TeV and that X has an interaction rate that can lead to signals at both collider detectors and direct and indirect detection experiments.

Freeze-In provides another general production mechanism and results when the interactions of X are insufficient to bring it into thermal equilibrium. At temperatures T above  $m_X$  these feeble interactions allow the production of X from decays or scatterings of some bath particle B of mass  $m_B$  at rate  $\Gamma(T)$ . This produces a yield of X particles at time  $t(T)$  of

$$Y_X^{Prod}(T) \sim \Gamma(T)t(T) \quad (2.1)$$

which is IR dominated when the interactions between B and X are of dimension 4 or less. Taking B to be the lightest observable sector particle carrying the stabilizing symmetry, the production rate becomes Boltzmann suppressed below  $m_B$ , so that the dominant contribution to  $Y_X$  arises at  $\sim m_B$ . For  $T > m_B$ , the yield  $Y(X)$  grows towards its equilibrium value, but it never reaches equilibrium, and this Freeze-In towards equilibrium stops once T drops below  $m_B$ . Decays

generally dominate over scatterings, so that in this paper we study the reaction

$$B \rightarrow A_{SM}X \quad (2.2)$$

where  $A_{SM}$  is one or more Standard Model particles.

It is assumed that Freeze-In (FI) production of dark matter during the early MD era via the decay  $B \rightarrow A_{SM}X$ .  $B$  is the lightest observable sector particle that carries the stabilizing symmetry,  $X$  is the dark matter and  $A_{SM}$  is one or more Standard Model particles. In addition to FI, there is a Freeze-Out (FO) population of  $B$  that eventually decays to  $X$ .

The number density evolution of  $X$  is described by the Boltzmann equation

$$\frac{dn_X}{dt} + 3Hn_x = \Gamma_B n_B^{eq} \frac{K_1[m_B/T]}{K_2[m_B/T]}, \quad (2.3)$$

with  $\Gamma_B$  the width of  $B$  and  $K_{1,2}[x]$  the first and second modified Bessel functions of the 2nd kind. The equilibrium number density obtained using Maxwell-Boltzmann statistics reads

$$n_B^{eq} = \frac{g_B}{2\pi^2} m_B^2 T K_2[m_B/T]. \quad (2.4)$$

At high temperatures ( $T \gg m_B$ ) we recover the  $T^3$  abundance for a relativistic species, whereas at low temperatures ( $T \ll m_B$ ) the number density has the Maxwell-Boltzmann exponential suppression. For this reason, the FI production of  $X$  is dominated at temperatures  $T_{FI} \simeq m_B$ .

If FI occurs during the RD era, the Boltzmann equation (2.1) can be easily solved giving a final yield for  $X$

$$Y_X = \frac{n_X}{s} = 4.4 \cdot 10^{-12} \left(\frac{g_B}{2}\right) \left(\frac{106.75}{g_*}\right)^{3/2} \left(\frac{300\text{GeV}}{m_B}\right) \left(\frac{\Gamma_B/m_B}{1.8 \cdot 10^{-25}}\right) \quad (2.5)$$

where  $s$  is the entropy density. Observations fix the DM density but the yield is fixed once the mass of  $X$  is known using

$$\xi_{DM} = \frac{\rho_{DM}}{s} = m_{DM} Y_{DM} = 0.44 \text{ eV} \quad (2.6)$$

which is close to the usual temperature of matter radiation equality,  $T_{eq} \simeq 1 \text{ eV}$ . We can thus rewrite eq. (2.5) as

$$\xi_X = \xi_{DM} \cdot \left(\frac{g_B}{2}\right) \left(\frac{106.75}{g_*}\right)^{3/2} \left(\frac{m_X}{100 \text{ GeV}}\right) \left(\frac{300 \text{ GeV}}{m_B}\right) \left(\frac{\Gamma_B/m_B}{1.8 \cdot 10^{-25}}\right) \quad (2.7)$$

The coupling  $\lambda$ , defined by

$$\Gamma_B = \frac{\lambda^2}{8\pi} m_B, \quad (2.8)$$

must be very small to avoid overclosure. For the reference masses and number of spin states shown in (2.5) the observed DM density results for  $\lambda \simeq 2 \cdot 10^{-12}$ .

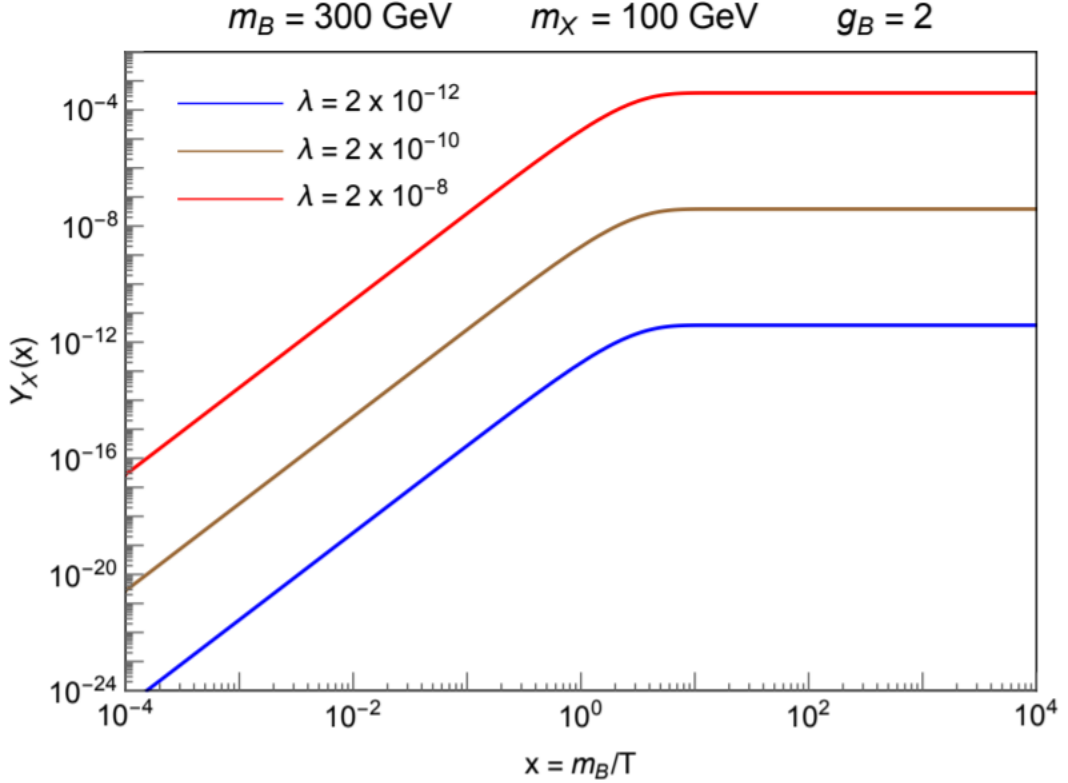


Figure 2.2: Yields  $Y_X(x)$  for FI during the RD era for three values of the decay width, as defined in Eq. (2.8), with fixed reference values  $m_B = 300 \text{ GeV}$ ,  $m_X = 100 \text{ GeV}$ , and  $g_B = 2$ .

In Fig.2.2 the FI solutions for the DM yield  $Y_X(x)$  are shown, with time variable  $x = m_B/T$ . There are three different lines corresponding to three different values of  $\lambda$  (namely three different decay widths as in Eq. (2.8)). In all cases we see that the process is maximally active at temperatures of order

$m_B$ . For the reference parameters of (2.5), the blue line reproduces the observed DM density, whereas the brown and red lines overproduce the amount of dark matter. In particular, the red line reaches an asymptotic value of  $Y_X$  which is 10 % the equilibrium value  $Y_X^{eq}$ , and above this point the approximation that DM arises from FI through the decay in Eq. (2.2), and without the inverse reaction, breaks down.

## 2.1. FREEZE-IN DURING NON-ADIABATIC EVOLUTION

Freeze-In during  $MD_{NA}$  occurs between  $a_{NA}$  and  $a_R$ , and the final DM density depends on only one parameter of the background, the reheat temperature  $T_R$ . This includes the important example of FI during reheating after inflation, as sketched in Fig. 2.1. In this case inflation could be the conventional one with more than 60 e-foldings with the matter M identified as the usual inflaton, or it could be a later era of inflation with fewer e-foldings.

The FI yields  $Y_X(x)$  are shown in Fig. 2.3 for three different values of the decay width

$$\lambda = \begin{cases} 2 \cdot 10^{-12} & T_R = 1TeV \\ 2 \cdot 10^{-8} & T_R = 4.6TeV \\ 2 \cdot 10^{-7} & T_R = 2.4TeV \end{cases} \quad (2.9)$$

In each case we choose  $T_R$  in such a way that we reproduce the observed DM abundance. The values of  $\lambda$  span a wider range than the case of Fig. 2.2 since Freeze-In during a MD era allows for larger couplings. The blue line has  $T_R > m_B$ , so that FI occurs during the RD era. As  $\lambda$  is increased, the FI process becomes more powerful, as illustrated by the brown and red lines, and to obtain the observed DM abundance much lower values of  $T_R$  must be taken, so that the X abundance is diluted by entropy production after FI. However, it is not possible to arbitrarily increase  $\lambda$  and still be in the Freeze-In regime. For sufficiently large  $\lambda$ , the peak of the  $Y_X$  functions in Fig. 2.3 will reach the equilibrium value and FI is no longer the applicable production mechanism. For reference values  $m_B = 300$  GeV,  $m_X = 100$  GeV, and  $g_B = 2$ ) this gives

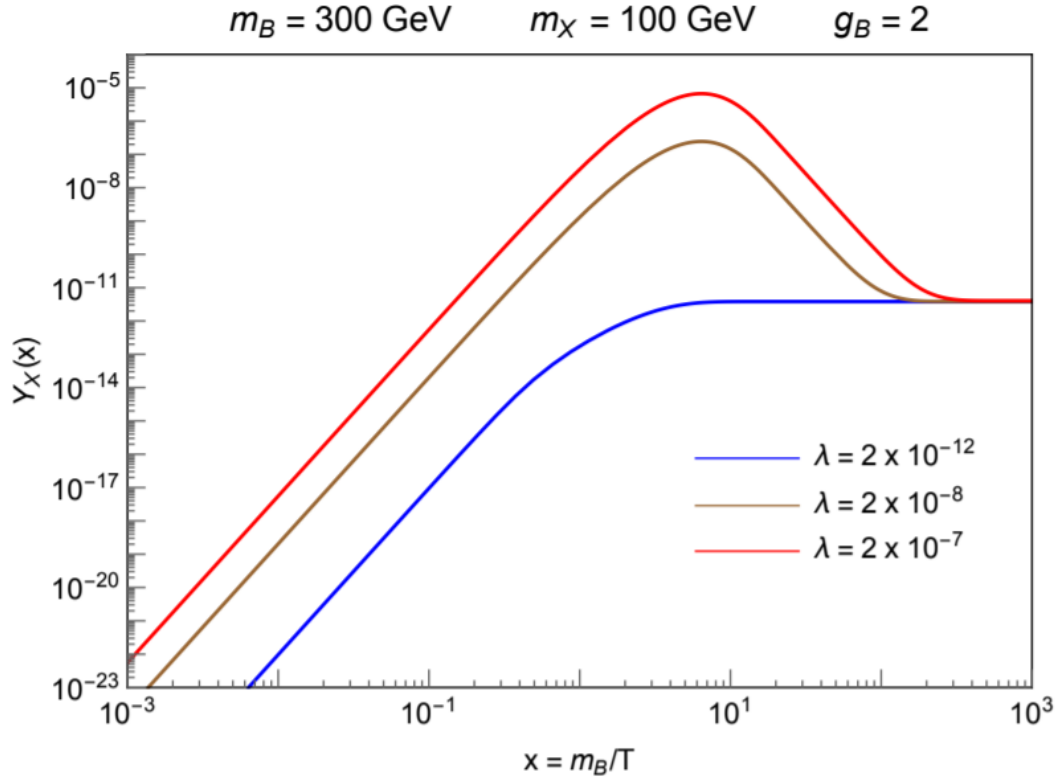


Figure 2.3: Yields  $Y_X(x)$  for FI during the  $MD_{NA}$  era, for example during reheating after inflation. For each of three  $\lambda$ ,  $T_R$  is chosen to give the observed DM abundance with fixed reference values  $m_B = 300 \text{ GeV}$ ,  $m_X = 100 \text{ GeV}$ , and  $g_B = 2$ .

a lower limit  $T_R \geq 0.6 \text{ GeV}$ . At the same time we have to keep  $T_R \leq m_B$ ; otherwise FI occurs during the RD era and there would be no dilution.[2]

### 3. NON-THERMAL PRODUCTION

There is increasing evidence that conventional cold dark matter (CDM) models lead to conflicts between observations and numerical simulations of dark matter halos on sub-galactic scales. Spergel and Steinhardt showed that if the CDM is strongly self-interacting, then the conflicts disappear. However, the assumption of strong self-interaction would rule out the favored candidates for CDM, namely weakly interacting massive particles (WIMPs), such as the neutralino.

There is strong evidence for the existence of a substantial amount of cold dark matter (CDM). The leading candidates for CDM are weakly interacting massive particles (WIMPs), such as the neutralino. The neutralino is the lightest supersymmetric particle. In models with R parity it is stable, and its mass density in the universe is generally assumed to be a relic of an initially thermal distribution in the hot early universe. Assuming, in addition, the presence of a small cosmological constant, the CDM scenario is consistent with both the observations of the large scale structure of the universe ( $\gg 1\text{Mpc}$ ) and the fluctuations of the cosmic microwave background. Many experiments searching for neutralino dark matter particles are under way.

The collisionless CDM scenario, however, predicts too much power on small scales, such as a large excess of dwarf galaxies, the over-concentration of dark matter in dwarf galaxies and in large galaxies. Recently Spergel and Steinhardt proposed a new concept of dark matter with strong self interaction. This puts WIMPs as candidates for dark matter in considerable jeopardy.

It is possible to propose a scenario with non-thermal production of WIMPs. These WIMPs could be relativistic when generated. Their comoving free-streaming scales could be as large as of the order 0.1 Mpc or larger. The density fluctuations on scales less than the free-streaming scale would then be severely suppressed. Consequently the discrepancies between the observations of dark matter halos on the sub-galactic scales and the predictions of the standard WIMPs dark matter picture could be resolved.

To begin with, supposed that a general case of non-thermal production of the neutralinos by the decay of topological defects such as cosmic string, by the decay of an unstable heavy particle, or produced non-thermally by the reheating process in a scenario of inflation at low energy scale. The momentum distribution function of the neutralinos is for simplicity assumed to be Gaussian:

$$f(p) = \frac{A}{\sqrt{2\pi}\sigma} \exp\left(-\frac{(p - p_c)^2}{2\sigma^2}\right), \quad (3.1)$$

where  $p_c$  is the central value and  $\sigma$  describes the width of the distribution.

Given a model, the parameters  $p_C$  and  $\sigma$  can be determined. For instance, in the supersymmetric version of the  $U_{B-L}(1)$  model, the (Higgsino-like) neutralinos arise directly from the decay of the right-handed neutrinos and their superpartners. In this model,  $p_C$  is about a half of the mass of the mother particles. For a two-body decay, if the mother particle is at rest, the distribution function  $f(p)$  is a  $\delta$ -function. The value of  $\sigma$  characterizes the average non-vanishing velocity of the mother particles (when  $\sigma \rightarrow 0$ ,  $f(p)$  approaches a  $\delta$ -function).

In Eq.(3.1),  $A$  is a normalization factor determined by the energy density of the non-thermal component

$$\rho(NT) = 4\pi \int E(p)f(p)p^2 dp, \quad (3.2)$$

where  $E(p) = (p^2 + m^2)^{1/2}$  and  $m$  is the rest mass of the dark matter particle. Given that the physical momentum  $p(t)$  scales as the inverse of the cosmic scale factor  $a(t)$ , also define  $r = a(t)p(t)/m$ . During cosmic evolution  $r$  is a constant. Throughout this paper we set  $a(t_0) = 1$ , so  $r$  can be understood as the velocity of the particles at the present time (note that the dark matter particles are non-relativistic now even though they are relativistic when generated).

The comoving free-streaming scale  $R_f$  for the non-thermal particles can be calculated as follows:

$$\begin{aligned}
R_f &= \int_{t_i}^{t_{eq}} \frac{v(t')}{a(t')} dt' \simeq \int_0^{t_{eq}} \frac{v(t')}{a(t')} dt' \\
&\simeq 2r_c t_{eq} (1 + z_{eq})^2 \ln \sqrt{1 + \frac{1}{r_c^2 (1 + z_{eq})^2} + \frac{1}{r_c (1 + z_{eq})}}
\end{aligned} \tag{3.3}$$

where  $r_c \equiv a(t)p_c(t)/m = p_c(t_0)/m$  and the subscript ' $_{EQ}$ ' denotes radiation-matter equality. Below the free-streaming scale, the power spectrum will be severely damped. To account for the lack of substructure in the Local Group, N-body simulations study show that the free-streaming scale of the dark matter should be  $\approx 0.1$  Mpc. This corresponds to  $r_c \approx 10^{-7}$ , which gives rise to a constraint on the parameters of the model.

The model with non-thermal production of WIMPs provides a promising scenario for large-scale structure formation of the universe. However, consistency needs to be checked with observations on small scales, especially on scales of the Lyman- $\alpha$  forest. In Fig. 3.1 shown the power spectrum of this model and the observed power spectrum of the Lyman- $\alpha$  system at  $z = 2.5$  shown as the filled circles with error bars. For comparison the power spectra for the conventional CDM and WDM models also given. In fitting to the observed data, the primordial spectral index  $n = 0.97$  for all models was chosen. The mass for the WDM particles is chosen as 750 eV, and the parameters for the NTDM models are  $r_c = (1.3, 1.4, 1.5) \cdot 10^{-7}$ , respectively.

For a flat universe with  $\Omega_\Lambda = 0.6$  the range of these scales corresponds to  $0.4h^{-1}Mpc \leq k \leq 12.8h^{-1}Mpc$ . From Fig. 3.1 one can see that the larger the value of  $r_c$  is, the lower the small-scale power spectrum becomes. By comparing the values of the power spectra at the upper limit of the above range in  $k$  with the power spectrum of the WDM model with  $m_W = 750$  eV, an upper limit on  $r_c$  of  $r_c \leq 1.5 \cdot 10^{-7}$  was obtained.

There were studies another constraints. The particle phase-space density  $Q$  is defined as  $Q \equiv \rho / \langle v^2 \rangle^{3/2}$ , where  $\rho$  is the energy density and  $\langle v^2 \rangle$  is the mean square value of the particle velocity. The astronomically observable quantity is the mean coarse-grained phase-space density. In the absence of dissipation, the coarse-grained phase space density can only decrease from its primordial

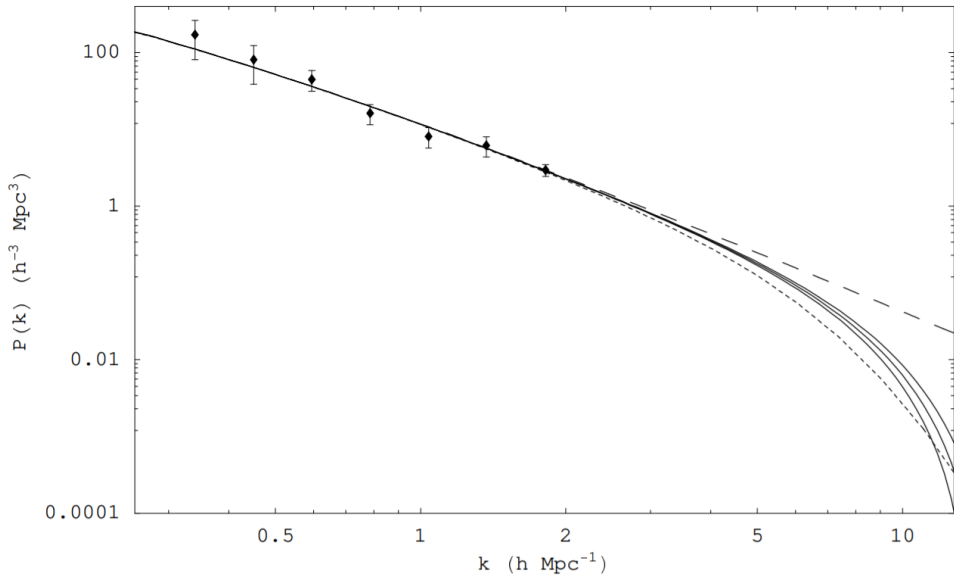


Figure 3.1: The power spectra of the CDM model (long dashed curve), the WDM model with  $m_W = 750$  eV (short dashed curve) and the NTDM models with  $r_c = (1.3, 1.4, 1.5) \cdot 10^{-7}$  (solid curves, from top down), compared to the observed Lyman- $\alpha$   $P(k)$  at  $z = 2.5$  (filled circles with error bars).

value. Thus, one can use the observed maximum phase-space density to set a lower limit on the phase-space density for the dark matter particles. The highest observed phase-space density is obtained from dwarf spheroidal galaxies:  $Q_{obs} \approx 10^{-4} M_{\odot} pc^3 (km/s)^{-3}$ . For these models,  $\langle v^2 \rangle \simeq r_c^2$  at the present time, and therefore

$$Q_0 \simeq \rho_{NT0}/r_c^3. \quad (3.4)$$

Because the primordial phase space density decreases with time when the particles are relativistic and becomes a constant after the particles become non-relativistic, one requires  $Q_0 > Q_{obs}$ , which can be translated into a constraint on  $r_c$ :

$$r_c < (\rho_{NT0}/Q_{obs})^{1/3} \approx 2.5 \cdot 10^{-7}. \quad (3.5)$$

This limit is of the same order of magnitude but slightly weaker than that from the observations of the Lyman- $\lambda$  forest.

Compared to the conventional CDM model, the power spectrum of this model on sub-galactic scales is severely damped, which will account both for the lack of substructure in the Local Group and for the observed smooth inner ha-

los. In addition, during the structure formation, the non-vanishing velocity of the WIMPs may further reconcile the discrepancies between the theoretical predictions and observations on sub-galactic scales. To solve the sub-galactic-scale problem, this model requires the value  $r_c \approx 1.5 \cdot 10^{-7}$ . This has implications on the models of non-thermal production of WIMPs.

In summary, the discrepancies between theory and observations on sub-galactic scales disfavours the conventional WIMPs CDM model. In this section we showed that if the dark matter particles have a non-thermal origin, these discrepancies can be resolved and the WIMPs remain good candidates for the dark matter particle.[\[3\]](#)

## 4. CANNIBAL DARK MATTER

A thermally decoupled hidden sector of particles, with a mass gap, generically enters a phase of cannibalism in the early Universe. The Standard Model sector becomes exponentially colder than the hidden sector. We propose the Cannibal Dark Matter framework, where dark matter resides in a cannibalizing sector with a relic density set by 2-to-2 annihilations. Observable signals of Cannibal Dark Matter include a boosted rate for indirect detection, new relativistic degrees of freedom, and warm dark matter.

In the non-relativistic dark matter class of models, under the generic requirement that number changing interactions are active, the hidden sector undergoes a phase of cannibalism. The properties of cannibalism are determined by the requirement that the dark sector and SM separately preserve their comoving entropy densities. This leads to different scalings of the temperature versus the scale factor  $a$ ,

$$T_\gamma \approx 1/a \quad \text{and} \quad T_d \approx 1/\log(a) \quad (4.1)$$

where  $T_\gamma(T_d)$  represents the temperature of the SM (cannibalizing) sector. The hidden sector temperature stays almost constant as the Universe expands as number changing interactions efficiently convert the rest mass of non-relativistic particles into kinetic energy. The different dependence on the scale factor implies that the SM particles are exponentially colder than the cannibalizing sector, as a function of the hidden sector temperature. In first studies and followup studies with cannibalism, it is assumed that DM annihilates through a 3-to-2 (or 4-to-2) process. Previous studies of cannibalism assume that the DM relic density comes from number changing interactions, such as 3-to-2 or 4-to-2 annihilations. In this section proposed a new class of DM models, where DM resides in a cannibalizing sector with relic density determined by 2-to-2 annihilations. In general, cannibal dark matter is realized in hidden sectors that contain both metastable states,  $\phi$ , undergoing number changing interactions such as  $\phi\phi\phi \rightarrow \phi\phi$ , and a stable DM candidate,  $\chi$ , annihilating into the

metastable states through 2-to-2 annihilations,  $\chi\chi \rightarrow \phi\phi$ .

The exponential cooling of the SM, during cannibalism, has dramatic implications for DM phenomenology. DM must have a larger annihilation rate than conventional scenarios, in order to reproduce the observed relic density. Therefore, Cannibal DM predicts boosted rates for indirect detection. The Universe is exponentially older at DM freeze-out, implying less redshifting between DM decoupling and the start of structure formation and therefore the possibility of warm DM. Cannibal DM can also lead to new relativistic degrees of freedom, leaving imprints on the Cosmic Microwave Background (CMB).

Cannibalism requires the following conditions:

- The dark sector is kinetically decoupled from the SM sector.
- The dark sector has a mass gap.
- The dark sector remains in chemical equilibrium, through number changing interactions, at temperatures below the mass of the LDP.

As a simple example, we consider a dark sector with a real scalar LDP (Lightest Dark sector Particle) and generic interactions,

$$V_\phi = \frac{m_\phi^2}{2}\phi^2 + \frac{A}{3!}\phi^3 + \frac{\lambda}{4!}\phi^4, \quad (4.2)$$

where  $A = \sqrt{3\lambda}m_\phi$ . Cannibalism begins when  $T_d$  drops below  $m_\phi$ , and chemical equilibrium is maintained through  $\phi\phi\phi \rightarrow \phi\phi$  annihilations.

In the following, we assume that  $\phi$  is metastable and eventually decays to either SM states or dark radiation.

In order for cannibalism to occur,  $\phi$  must be out of kinetic equilibrium with its decay products and therefore have lifetime longer than Hubble,  $\tau_\phi > H^{-1}$ , when  $T_d = m_\phi$ . For decays to SM, we focus on  $\phi \rightarrow \gamma\gamma$ . For the dark radiation case, we assume that  $\phi$  decays to a light species that is kinetically decoupled from  $\phi$  and begins with zero abundance (for example  $\phi \rightarrow \gamma'\gamma'$ , where  $\gamma'$  is a light hidden photon).

Since the dark sector and the SM are kinetically decoupled, they have different temperatures and entropies. Assuming for simplicity that there are no entropy injections, the comoving entropies of the two sectors are separately conserved. This implies that the ratio of SM to dark entropy densities is fixed,

$$\xi \equiv \frac{s_{SM}}{s_d}. \quad (4.3)$$

If the two sectors were in thermal contact in the past,  $\xi$  is the ratio of the sum of degrees of freedom within each sector. However,  $\xi$  can be much larger if the two sectors reheat to asymmetric temperatures and remain thermally decoupled.

During cannibalism,  $T_d$  and  $s_d$  are related,

$$s_d \equiv \frac{2\pi^2}{45} g_{*s}^d T_d^3 \simeq \frac{m_\phi^3}{(2\pi)^{3/2} x_{phi}^{1/2}} \exp -x\phi \quad (4.4)$$

where  $x_\phi \equiv m_\phi/T_d$  and we assume, for simplicity, that  $\phi$  dominates the hidden sector entropy. Conservation of entropy within each sector implies that the SM becomes exponentially colder than the dark sector.

# REFERENCES

- [1] L. Baudis and S. Profumo. “Dark Matter”. In: (2019), p. 31.
- [2] Raymond T. Co et al. “Freeze-In Dark Matter with Displaced Signatures at Colliders”. In: (2015), p. 26.
- [3] W.B. Lin et al. “Non-Thermal Production of WIMPs and the Sub-Galactic Structure of the Universe”. In: (2000), p. 6.